

A Rapid Forecasting and Mapping System of Storm Surge and Coastal Flooding

KUN YANG, VLADIMIR A. PARAMYGIN, AND Y. PETER SHENG

Department of Civil and Coastal Engineering, University of Florida, Gainesville, Florida

(Manuscript received 16 July 2019, in final form 2 March 2020)


ABSTRACT

A prototype of an efficient and accurate rapid forecasting and mapping system (RFMS) of storm surge is presented. Given a storm advisory from the National Hurricane Center, the RFMS can generate a coastal inundation map on a high-resolution grid in 1 min (reference system Intel Core i7-3770K). The foundation of the RFMS is a storm surge database consisting of high-resolution simulations of 490 optimal storms generated by a robust storm surge modeling system, Curvilinear-Grid Hydrodynamics in 3D (CH3D-SSMS). The RFMS uses an efficient quick kriging interpolation scheme to interpolate the surge response from the storm surge database, which considers tens of thousands of combinations of five landfall parameters of storms: central pressure deficit, radius to maximum wind, forward speed, heading direction, and landfall location. The RFMS is applied to southwest Florida using data from Hurricane Charley in 2004 and Hurricane Irma in 2017, and to the Florida Panhandle using data from Hurricane Michael in 2018 and validated with observed high water mark data. The RFMS results agree well with observation and direct simulation of the high-resolution CH3D-SSMS. The RFMS can be used for real-time forecasting during a hurricane or “what-if” scenarios for mitigation planning and preparedness training, or to produce a probabilistic flood map. The RFMS can provide more accurate surge prediction with uncertainties if NHC can provide more accurate storm forecasts in the future. By incorporating storms for future climate and sea level rise, the RFMS could be used to generate future flood maps for coastal resilience and adaptation planning.

1. Introduction

Florida, with 1350 mi of coastline, is highly prone to landfalling hurricanes. Between 1851 and 2018, 126 hurricanes struck Florida, 40 of which are major hurricanes, and southwest Florida recorded 16 major hurricanes, which is the most for any individual area in the United States (Wikipedia 2019; Blake et al. 2011). Hurricane Irma (2017) is the costliest hurricane [\$65 billion (U.S. dollars)] for Florida, followed by Wilma (2005), Andrew (1992), Ivan (2004), and Michael (2018). To enable state and local governments to develop more effective evacuation plans before a hurricane landfall, it is essential to quickly produce and provide accurate coastal inundation maps to the local emergency managers. Currently, local emergency managers rely on the Surge Atlas [aka maximum of the maximum (MOM; NHC 2019)], which represents the likely maximum

inundation for specific coastal regions, and the real-time surge forecast provided by the National Hurricane Center (NHC) for evacuation planning. Although the NHC forecasts are provided quickly, their forecast of overland flooding does not provide sufficient accuracy, due to the relatively simple physics (e.g., linear dynamics, empirical bottom friction, lack of wave effects) and the typically coarse grid resolution (>1000 m) of the numerical hydrodynamic model, Sea, Lake, and Overland Surge from Hurricanes (SLOSH; see, e.g., Jelesnianski et al. 1992; Forbes et al. 2014a). Nevertheless, SLOSH is computationally very efficient as it takes only 2–3 min to complete a hurricane surge forecast (reference system is a single-CPU, Intel Core i7-3770K). SLOSH uses storm parameters, such as storm center location, central pressure deficit, size, and forward speed to generate wind fields and its surge forecast result is usually accurate to within $\pm 20\%$ of observed water level data according to NOAA/NWS/NHC (2013). Recent studies by Forbes et al. (2014a,b) used more refined grid ~ 350 m in some regions; however, its resolution is still significantly lower than needed to adequately represent flooding dynamics in complex urban environments.

 Denotes content that is immediately available upon publication as open access.

Corresponding author: Y. Peter Sheng, pete@coastal.ufl.edu

DOI: 10.1175/WAF-D-19-0150.1

© 2020 American Meteorological Society. For information regarding reuse of this content and general copyright information, consult the AMS Copyright Policy (www.ametsoc.org/PUBSReuseLicenses).

Typically, the NHC storm advisories are issued at 6-h intervals and storm surge forecast needs to be completed within 1 h after an advisory is issued (Condon et al. 2013). High-resolution, real-time storm surge forecasting systems that use high-fidelity hydrodynamic models such as Advanced Circulation Model (ADCIRC) (see, e.g., Luettich et al. 1992; Fleming et al. 2008; Mattocks and Forbes 2008), Finite Volume Coastal Ocean Model (FVCOM) (see, e.g., Chen et al. 2003; Rego and Li 2009), Curvilinear-Grid Hydrodynamics in 3D Storm Surge Modeling System (CH3D-SSMS) (see, e.g., Sheng et al. 2006, 2012a; Paramygin et al. 2017), and Princeton Ocean Model (POM) [see, e.g., Peng et al. (2004), or ECOM (Jordi et al. 2019) which is an extension of the POM] are all able to forecast hurricane-induced storm surges with high resolution of 100 m or less. For example, the high-resolution (>30 m), 3D storm surge forecast system CH3D-SSMS (Sheng et al. 2010; Paramygin et al. 2017) can complete a storm surge and coastal flooding forecast for southwest Florida in about 60 min on a reference computer system described earlier. Other high-resolution storm surge models could take several hours to complete the forecast on a similar computer platform. However, these forecasting systems are still computationally expensive compared to SLOSH, the two-dimensional low-fidelity (with low resolution and simple physics) storm surge model used by the NHC. A detailed comparison of five storm surge models (ADCIRC, CH3D, FVCOM, POM, and SLOSH), in terms of their accuracy and efficiency, for simulating historical storm and producing probabilistic coastal inundation maps and surge atlas is described in Sheng et al. (2010). As models become more robust in physics (e.g., including tides and wave effects on surge) and model grid resolutions increase, their computational costs also increase significantly.

At the same time, the growth in processor speed has slowed down tremendously. Therefore, the need to complete forecasts quickly using a high-fidelity model with robust physics and high grid resolution becomes a challenging task. For example, hundreds to thousands of processors may be needed to run a high-fidelity model forecast cycle, and even more processors may be needed if simultaneous ensemble forecasting for a large storm ensemble is performed to address the uncertainties associated with storm and surge forecast errors. Computational efficiency (albeit simpler physics and lower resolution) is the main reason that SLOSH is still the model of choice for the National Hurricane Center. Therefore, to achieve the goal of accurate and efficient forecasting of coastal inundation for improved emergency planning, it is necessary to explore an alternative method which combines the accuracy of a direct

forecasting system based on a high-fidelity model and the efficiency of a direct forecasting based on a low-fidelity system.

Local emergency managers rely on the SLOSH-based real-time surge forecasts, as well as the nonprobabilistic surge atlas, for evacuation and mitigation planning. While these products have been effective in minimizing flood damage in coastal regions, local emergency managers have expressed desires for more accurate products which are obtained with high-fidelity models. More accurate inundation forecasts and maps can reduce the evacuation cost during a hurricane. Additionally, coastal communities rely on the 1% annual exceedance probability (AEP) coastal inundation maps produced by FEMA (FEMA 2019; NRC 2009; Condon and Sheng 2012; Yang et al. 2019) for resilience and adaptation planning. However, the FEMA flood maps are only updated every five or more years to incorporate changes in storms statistics and land use features. Moreover, the effects of changing climate and accelerating sea level rise on coastal flooding are not incorporated into the FEMA flood maps. To enable the production of more accurate and frequently updated flood maps, surrogate modeling using high-fidelity models can be applied as described in Condon and Sheng (2012) and Yang et al. (2019). The surrogate modeling technique developed by Yang et al. (2019) is the foundation of the RFMS described in this paper. As such, the RFMS is proposed not only as a faster and more accurate forecasting system in this paper, but also a system that can be used to quickly produce and update probabilistic coastal flood maps more frequently than every 5–10 years, as shown in Yang et al. (2019). Computational details on flood map generation can be found in Condon and Sheng (2012) and Yang et al. (2019), hence will not be repeated in this paper. While there is similarity between the basic methods used in Yang et al. (2019) and this paper, the methods for optimal storm determination and kriging are made more efficient in this paper.

Recently, surrogate modeling has been used for storm surge forecasting. Surrogate modeling consists of two steps. In the preprocessing step, hundreds of direct model simulations are performed using a high-fidelity model. In the forecasting step, a surrogate model is used to interpolate the direct simulation results to quickly produce a forecast and inundation map. Condon et al. (2013) used multivariate adaptive regression spline (MARS) as a surrogate model with a predefined optimal storm database (obtained with CH3D-SSMS) to determine the inundation in southwest Florida during Hurricanes Charley and Wilma. Kim et al. (2015) used an artificial neural network (ANN) method and a database of 446 tropical storms to predict time series of

water level at 25 coastal locations in southern Louisiana. Jia et al. (2016) used the same 446 tropical storms as the database and kriging as the surrogate model to predict the peak surge response and surge time series at coastal stations. The predictions by Kim et al. (2015) and Jia et al. (2016), while efficient, focused only on water elevations at open water coastal stations but ignored inundation over typically dry land which becomes inundated only during storms. The drawbacks of ANN include difficulty in determining proper network structure, which is often achieved by trial and error, and the requirement that a relatively large dataset be available for training, validating and testing, in comparison to the surrogate modeling.

This paper builds a prototype/proof-of-concept of the rapid forecast and mapping system (RFMS) of storm surge and coastal flooding for local coastal communities. The RFMS can produce a high-resolution inundation map (envelope of maximum water elevation above ground) from a given storm forecast issued by the NHC in 1 min (reference system is a single-CPU, Intel Core i7-3770K), compared to the 5–8 min needed by the forecasting system in Condon et al. (2013), and the 60+ min needed by direct simulation using CH3D-SSMS.

The RFMS aims to provide supplemental high-resolution inundation forecast to local communities during hurricanes quickly and to allow local planning managers to develop what-if scenarios that can be expected for the coastal region (e.g., what if IRMA were to move 40 mi to the west of the storm track or Charley were to triple its size). This study improves the MARS interpolation method and the optimal storm selection process used by Condon et al. (2013) by using the quick kriging method and a database of 490 objectively selected optimal storms. To validate its accuracy and efficiency, the RFMS is evaluated by hindcasting the storm surge and coastal inundation in southwest Florida during Hurricanes Charley and Irma and in Florida Panhandle during Hurricane Michael using best track data provided by the NHC. Simulated results are compared with the observed surge in open water and high water marks (HWMs) on land.

While nonparametric hurricane wind models such as H*Wind (Powell et al. 1998) and WRF (Powers et al. 2017) are capable of producing accurate wind fields, they are also computationally demanding and require an excessive amount of time to produce real-time forecasts, which adds to the total time required to produce a storm surge forecast. The RFMS currently employs the Holland (1980) parametric wind model, for simplicity, to generate a hurricane wind field from a set of

parameters provided by the NHC storm forecasts. While the Holland model is capable of simulating historical storms (e.g., Vickery et al. 2000; Condon et al. 2013), it contains a few limitations (e.g., lack of wind field asymmetry, which becomes especially important in the northern parts of the United States as storms undergo extratropical transition). Thus the prototype RFMS has a few limitations inherited from the Holland (1980) model, as well as the use of a set of parameters (location of storm center, central pressure deficit, radius to maximum wind, translational speed, and angle of approach at landfall) as model inputs, which are discussed in section 5. Central pressure deficit is used as the main predictor of storm intensity and radius to maximum wind as a measure of storm size. For simplicity, the system discussed in the paper does not include the effects of astronomical tides, which can be added in the future, as discussed in more detail in section 4. While all these can be viewed as simplifying approximations of the proposed prototype system, the proposed surrogate modeling approach is found to yield more accurate and efficient forecasts over SLOSH. The set of input parameters can be changed, parameter quantization can be refined, and Holland model can be replaced with a different parametric wind model [e.g., Xie et al. (2006) or Bao et al. (2006)]. The asymmetric hurricane wind model by Xie et al. (2006) uses wind radii of 34, 50, and 64 kt ($1 \text{ kt} \approx 0.51 \text{ m s}^{-1}$) winds for the four quadrants of the wind field. Although this would increase the dimension of input parameters, which may significantly increase the number of optimal storms (discussed in section 3), the fundamental methodology and computing efficiency during the forecast cycle would remain the same.

In the following sections, we present the basic hydrodynamic modeling system and the model domains (section 2), the surrogate model forecasting method of the RFMS (section 3), applications of the RFMS in southwest and northwest (the Panhandle) Florida (section 4), uncertainty analysis of kriging interpolation (section 5), RFMS results based on NHC forecast advisories (section 6), and summary and conclusions (section 7). It should be noted that, while this paper addresses the uncertainties of the surrogate model-based forecasting, it does not attempt to address the general uncertainties of storm-track predictions or storm surge model simulations as described by Sheng in the NRC (2009) report.

2. Hydrodynamic models and model domains

Two hydrodynamic models: SLOSH and CH3D, are used in the RFMS. SLOSH, as illustrated in section 3,

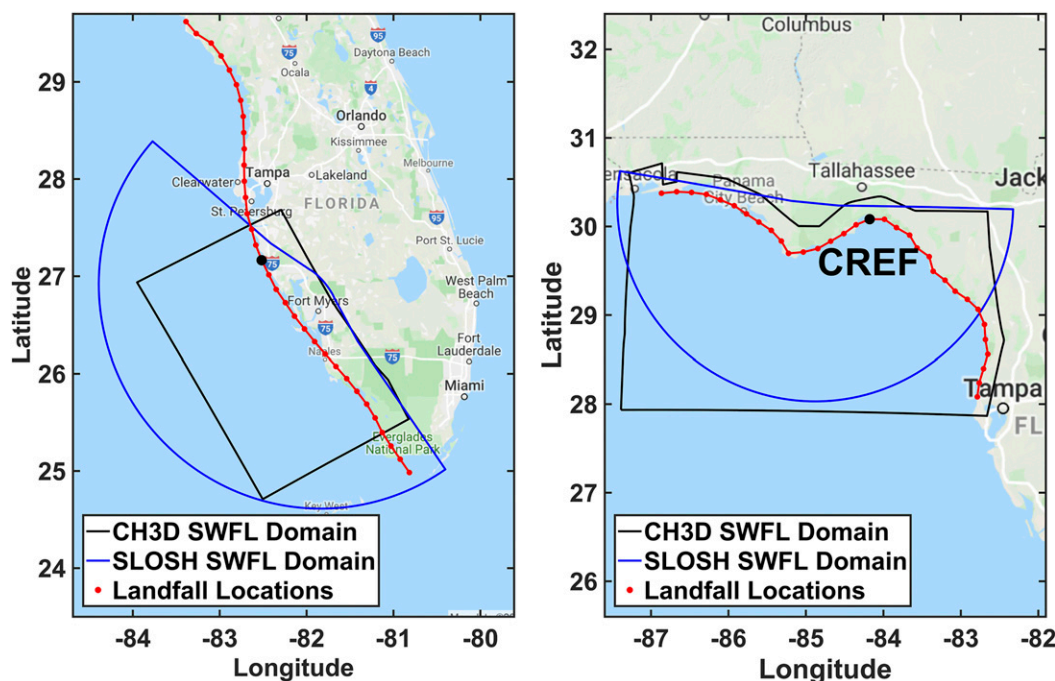


FIG. 1. CH3D domain (black), SLOSH domain (blue), simplified coastline (red), and CREF for (left) southwest Florida and (right) Florida Panhandle.

is used for selecting the optimal storms for RFMS. Condon et al. (2013) showed that SLOSH can be very effectively used in selecting the optimal storms by the joint probability method with optimal sampling (JPMOS). Once the optimal storms are selected, the latest version of the CH3D model (Sheng 1987, 1990) is used as the high-resolution hydrodynamic model to evaluate the storm surge for each storm and build the database. CH3D uses a boundary-fitted, nonorthogonal curvilinear grid in the horizontal direction and terrain-following sigma grid in the vertical direction. CH3D is coupled to a wave model SWAN (Booij et al. 1999) to produce CH3D-SSMS (Sheng et al. 2006, 2010; Paramygin et al. 2017). To provide the water level at the open boundaries of the southwest Florida domain for CH3D, output of a regional-scale ADCIRC model is used. For simplicity, this study uses the 2D version of CH3D and the bottom friction is calculated using a spatially varying Manning's coefficient, which is determined from U.S. Geological Survey (Sugarbaker and Carswell 2011). A detailed description of the model domains can be found in appendixes A and B in this paper, and the governing equations and boundary conditions can be found in appendix B of Condon et al. (2013). Figure 1 shows the CH3D-SSMS and SLOSH domains, simplified coastlines and the center of reference (CREF) for southwest Florida and Florida Panhandle. The CH3D model is forced by a parametric

tropical storm wind model (Holland 1980) that uses location of the storm, pressure deficit at the center, radius to maximum winds and translational speed of the storm to compute wind and pressure fields (the B shape parameter is calculated from these parameters and is bound between 1 and 2.5, and the A parameter is calculated from B and the radius to maximum wind).

3. Forecasting method of RFMS

The forecasting of storm surge using RFMS can be divided into two parts. The first part, the preprocessing step, is completed prior to the start of a hurricane season and includes selecting optimal storms from a large ensemble of test storms and then a high-fidelity model is used to simulate the surge during the optimal storms. Results of these simulations are then stored in a database. The second part, the forecasting step, is executed in real time by using a surrogate model to generate a flood map based on a given storm track issued by the NHC and the precomputed surge database of optimal storms.

a. Test storms

The storm surge due to a hurricane is mainly determined by five landfall parameters of hurricane (Irish et al. 2008; Jordan and Clayson 2008): central

pressure deficit P_c , radius to maximum wind R_m , storm forward speed V_f , storm heading direction θ , and landfall location L_0 . First, a range and discretization must be defined for each parameter. Following the method in Condon and Sheng (2012), 5 values are selected for each of the four parameters P_c, R_m, V_f, θ , and 33 values are selected for L_0 (shown in Table 1). The values are selected based on the historical data from hurricanes that affected southwest Florida (Condon and Sheng 2012) and Florida Panhandle between 1940 and 2018. A total of 20 625 ($=5^4 \times 33$) storms, which are called test storms, are defined by using all possible combinations of the selected parameter values, and storm tracks are generated for these synthetic storms based on these landfalling characteristics.

The test storms are then simulated with SLOSH, and total inundation volume (TIV) (Sheng et al. 2012b) for each storm is calculated by

$$TIV_j = \sum_{i=1}^{N_c} A_i \times H_{ij}, \quad j = 1, \dots, m, \quad (1)$$

where N_c is the number of land grid cells of the domain, A_i is the area of the land grid cell, H_{ij} is the inundation height of the i th land grid cell from j th storm, which is calculated by subtracting bottom elevation of the land cell from the simulated maximum envelope of water (MEOW) of the cell, and m is the total number of test storms. The TIV calculated from result of a direct simulation is called STIV. TIV is a good metric for coastal inundation as it is the product of total inundation area (TIA) and the average inundation height (AIH), as explained in Sheng et al. (2012b).

b. Optimal storm selection

To reduce the size of the storm database and interpolation time, the test storm ensemble needs to be reduced significantly below 20 625. A number of so-called *optimal storms* are selected from the test storms. The optimal storms and their responses then form the database to be used by quick kriging interpolation method. Briefly, the optimal storms are objectively selected in the following way:

- 1) Select 113 fundamental optimal storms. The fundamental optimal storms consist of 1) combinations of the maximum/minimum values of the five landfall parameters (32 fundamental optimal storms), 2) combinations of median value of one landfall parameter with the maximum/minimum values of the other four landfall parameters (80 fundamental optimal storms), and 3) combination of the median

TABLE 1. The values of the landfall parameters in RFMS for southwest Florida and the Florida Panhandle.

P_c (mb)	R_m (mi)	θ (°)	V_f (mi h ⁻¹)	L_0 (n mi)
Southwest Florida				
15	10	0	5	From -160 to 160 relative to CREF for every 10 n mi (33 locations)
35	40	22.5	10	
55	80	45	15	
75	120	67.5	20	
95	160	90	30	
Florida Panhandle				
15	10	-20	6	From -160 to 160 relative to CREF for every 10 n mi (33 locations)
35	25	0	13	
55	40	20	20	
75	55	40	27	
95	70	60	34	

values of the five landfall parameters (1 fundamental optimal storm).

- 2) Find the TIV of the optimal storms from the STIV. The storm surge responses to the test storms other than the optimal storms are interpolated from optimal storm responses using quick kriging technique, rather than simulated directly, and the TIV calculated from the results obtained by interpolation is combined with the TIV of the optimal storms, which is called ITIV.
- 3) The difference between STIV and ITIV, called DTIV, is calculated by

$$DTIV_j = |STIV_j - ITIV_j|, \quad j = 1, \dots, m. \quad (2)$$

- 4) Find the maximum value of DTIV and the corresponding storm from the test storms. Add that storm into the optimal storm set.
- 5) Calculate the averaged TIV error (ATE) as

$$ATE = \frac{1}{m} \sum_{j=1}^m \frac{DTIV_j}{STIV_j} \times 100\%. \quad (3)$$

- 6) Repeat steps 2–4, each time one more optimal storm is added into the optimal storm set, until the desired accuracy (ATE) is achieved.

Figure 2 shows ATE as a function of the number of optimal storms used in the RFMS. Based on this result, 490 optimal storms are selected with the desired ATE lower than 10%. The regression plot between STIV and ITIV is shown in Fig. 3, with coefficient of determination (R^2) of 0.98. The ATE and R^2 values indicate that every test storm could be accurately interpolated by the quick kriging technique with the database consisting of 490 optimal storms.

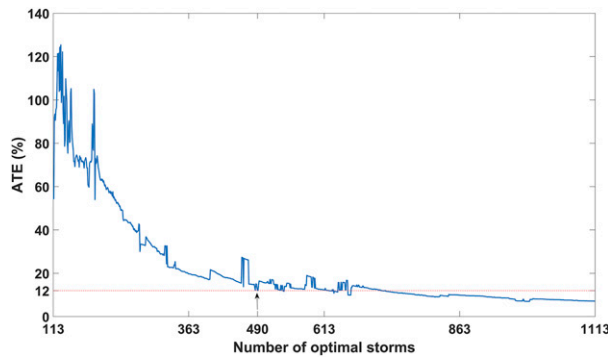


FIG. 2. The curve of ATE as a function of the number of optimal storms used in quick kriging interpolation.

c. Direct simulation

The optimal storms are simulated by the high-resolution CH3D-SSMS, and surge responses are saved to the database. Steps 1–3 prepare the system for forecasting and can be executed before the hurricane season starts. This allows the numerical models used for direct simulations to be as complex as necessary and have very high resolution since these simulations do not have the severe time constraint imposed by the NHC for the forecast cycles. Once the optimal surge database is generated, the system is ready for forecasting.

d. Surrogate model: Quick kriging interpolation method

During a forecasting cycle, the system receives a predicted storm track (e.g., from NHC) and uses this information combined with the predefined database to generate a flood map. The quick kriging (QK) method is used to interpolate the response of any storm defined by its landfall parameters. The kriging model is a Gaussian surrogate model, and the value at a point is weighted according to spatial covariance value and is correlated to the values at neighboring points. To generate the water level response of a storm for one domain, the kriging model could be trained at each cell inside the domain using the water level responses of the optimal storms and perform kriging interpolation for each cell. In this way, the number of interpolations needed equals to the number of cells in the domain. Alternatively, the kriging model could be trained using water level responses of all cells inside the domain once, then only one kriging interpolation is needed. The latter interpolation method could generate the water level responses for the whole model domain much faster with slightly less accurate results, compared to the former interpolation method. Therefore, the latter method, called quick kriging, is

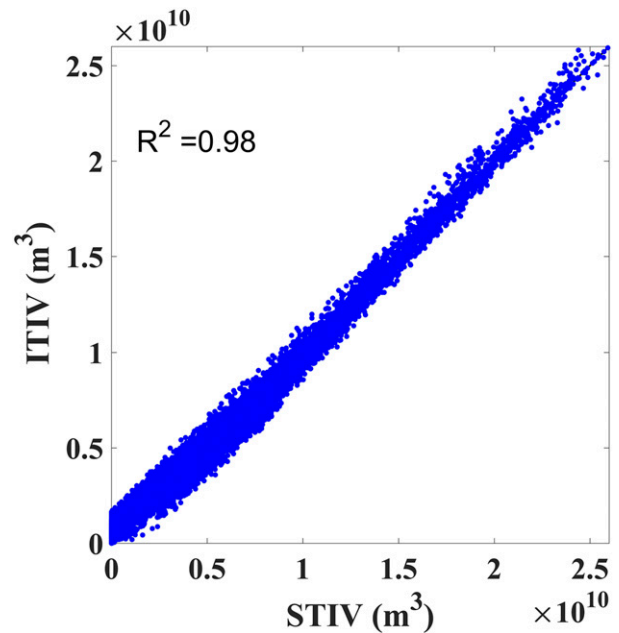


FIG. 3. Comparison between STIV and ITIV with 490 optimal storms.

adopted in this study because of its high efficiency. Yang et al. (2019) showed that the global kriging (RMSE = 0.17 and $R^2 = 0.95$) is only slightly less accurate than the local kriging (RMSE = 0.16 and $R^2 = 0.96$) and the difference between the two results is negligible, especially when compared to other uncertainties. More details of the two kriging methods and their accuracy and efficiency can be found in Yang et al. (2019).

The RFMS forecasting procedure is summarized as follows:

- 1) Receives the most recent tropical storm advisory that contains track information and storm characteristics;
- 2) Extracts/estimates the five storm parameters at landfall;
- 3) Uses the set of parameters from step 2 and optimal storm database to perform quick kriging interpolation and obtain interpolated water levels at every grid cell; and
- 4) Calculates inundation as interpolated water level minus land elevation at all output points and creates output in user-specified format (e.g., GIS-enabled raster GeoTIFF).

Details of the procedure are described graphically in appendix C. With the surge database of 490 optimal storms, the RFMS takes less than 1 min to generate an inundation map from an NHC forecast advisory, which gives the emergency managers much more time to make

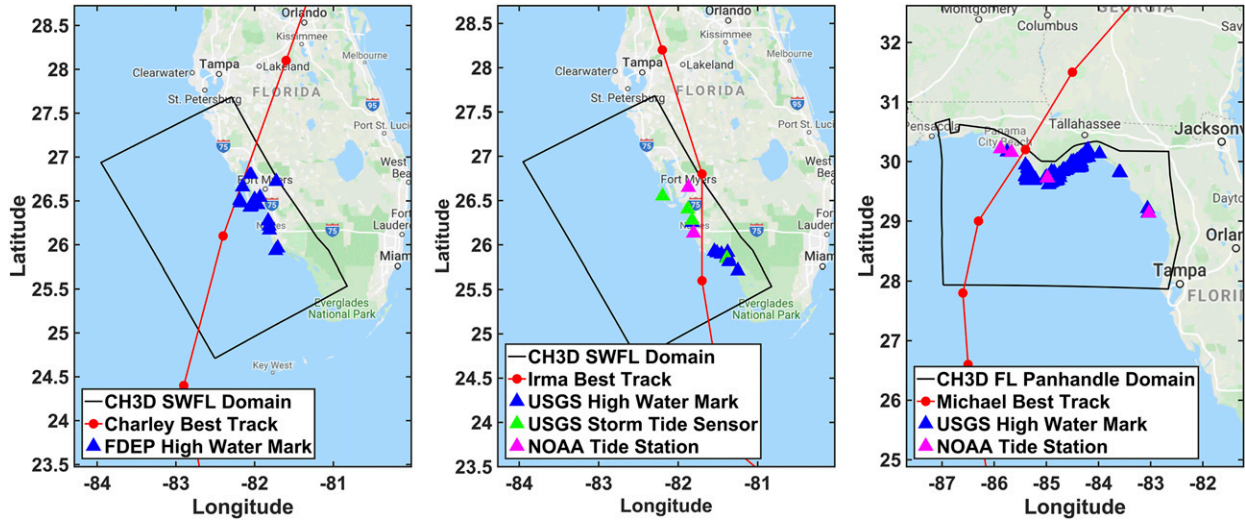


FIG. 4. The best track and the locations of HWMs of (left) Hurricane Charley, (center) Hurricane Irma, and (right) Hurricane Michael.

decisions than if CH3D-SSMS were used for forecasting. It also provides much more detailed and accurate coastal flooding information than SLOSH, as a supplement for emergency evacuation planning. The RFMS can also be used by planners in coastal governments to quickly produce flood maps of “what-if” scenarios and probabilistic maps with various return periods for adaptation and resilience planning. These maps can be overlaid onto maps of critical infrastructures in a GIS system to enable resilience and adaptation planning.

4. Application of the RFMS to southwest and northwest (Panhandle) Florida

The accuracy of the RFMS is evaluated by hindcasting Hurricane Charley, which was discussed in Condon et al. (2013), Hurricane Irma in 2017, and Hurricane Michael in 2018. Best tracks from the Atlantic hurricane database (HURDAT2) and locations of the HWMs of the three hurricanes are shown in Fig. 4. The best tracks are used instead of forecast tracks because the focus of the paper is not on the accuracy of the forecast track, but on the feasibility of the proposed RFMS. As pointed out by Condon et al. (2013), “Use of the tide model did not improve the results much but does nearly double the time needed to build the surge response”, thus the tide model is not included when applying the RFMS to the domains. Depending on the model domain and tidal amplitudes, tide may need to be considered by including more optimal storms with flood and ebb tides for all intermediate tidal amplitudes into the database. The exclusion of tide does not impact the results

noticeably due to the relatively low tidal range in Florida (Condon et al. 2013).

a. Hurricane Charley (2004)

Hurricane Charley made landfall near the peninsula in Punta Gorda, Florida on 13 August 2004. At the time of landfall, Charley was a very compact and a fast-moving storm, with landfall parameters: P_c of 72 mb (1 mb = 1 hPa), R_m of 11.5 mi, V_f of 21.6 mi h⁻¹, θ of 16.6°, and L_0 of -46 [46 n mi (1 n mi = 1.852 km) south of CREF]. Detailed descriptions of Hurricane Charley can be found in National Hurricane Center (2004). The inundation maps of Hurricane Charley simulated by CH3D-SSMS and interpolated by RFMS are shown in Fig. 5. The observed HWM data collected by the Florida Department of Environment Protection (FDEP) are compared to the simulated and interpolated peak water levels in Fig. 5. The interpolated peak water levels have R^2 of 0.70 and slightly lower RMSE (0.37 m) than simulated peak water levels (0.40 m), compared to the observed HWM data. Hurricane Charley is then simulated by SLOSH and the simulated peak water levels are compared to the observed HWM data in Fig. 5. The RMSE of 0.63 m and R^2 of 0.16 indicate that the directly simulated results by SLOSH are much less accurate than the direct simulated results by CH3D and interpolated results by RFMS.

The HWM comparison between observed water levels and interpolated water level, with R^2 of 0.70, is better than that the value of 0.55 in Condon et al. (2013). This is expected, as the water level response produced by kriging interpolation method is more accurate than that by multivariate interpolation

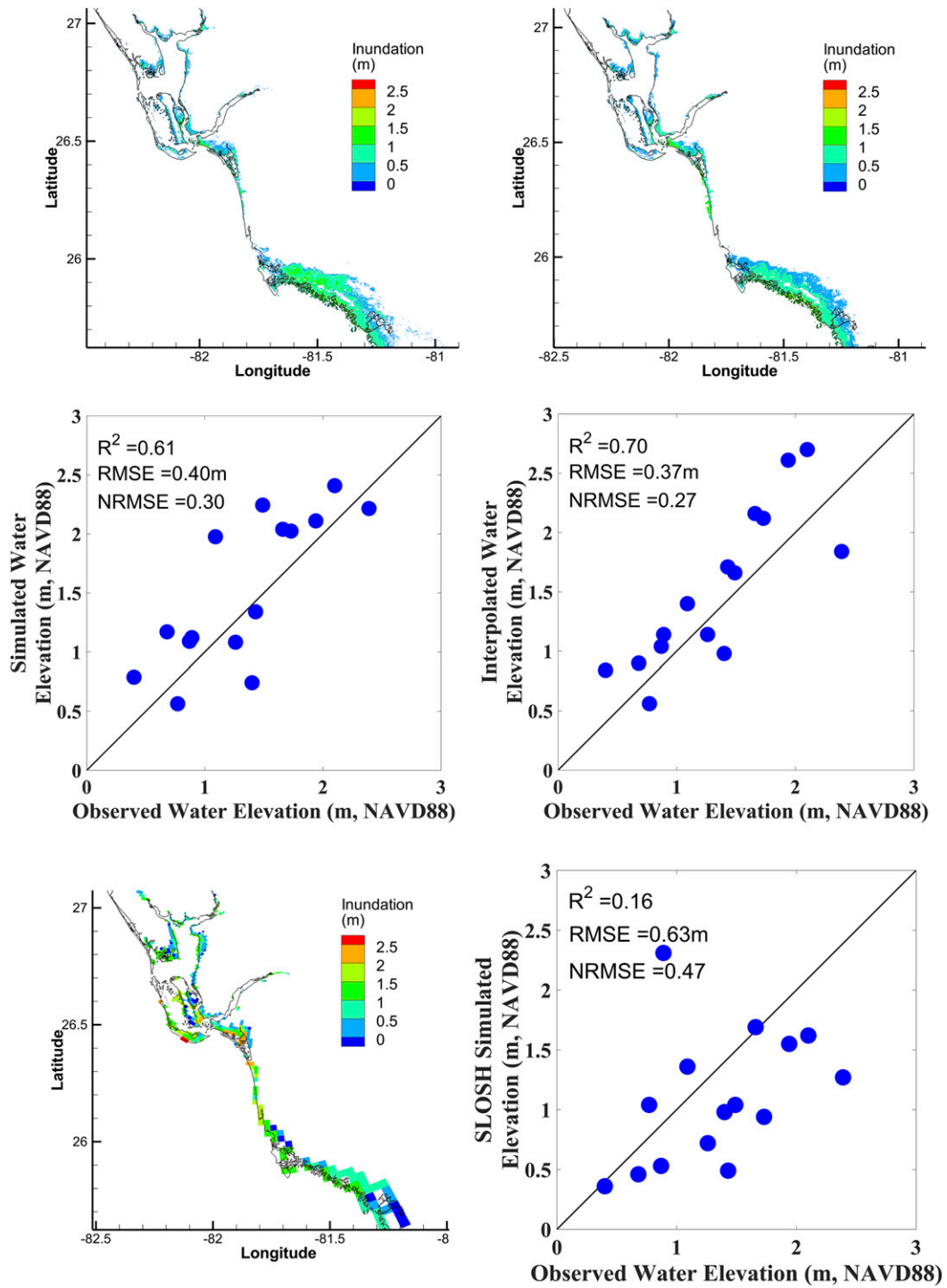


FIG. 5. Inundation maps (top left) simulated by CH3D-SSMS, (top right) interpolated by RFMS, and HWM comparisons between observed water elevations and (middle left) simulated water elevations by CH3D-SSMS, and (middle right) interpolated water elevations by RFMS for Hurricane Charley. (bottom left) Inundation map simulated by SLOSH and (bottom right) HWM comparisons between observed water elevations and simulated water elevations by SLOSH during the stage of peak water level. Blue circles represent the FDEP high water mark data. RMSE is root-mean-square error and NRMSE is normalized root-mean-square error.

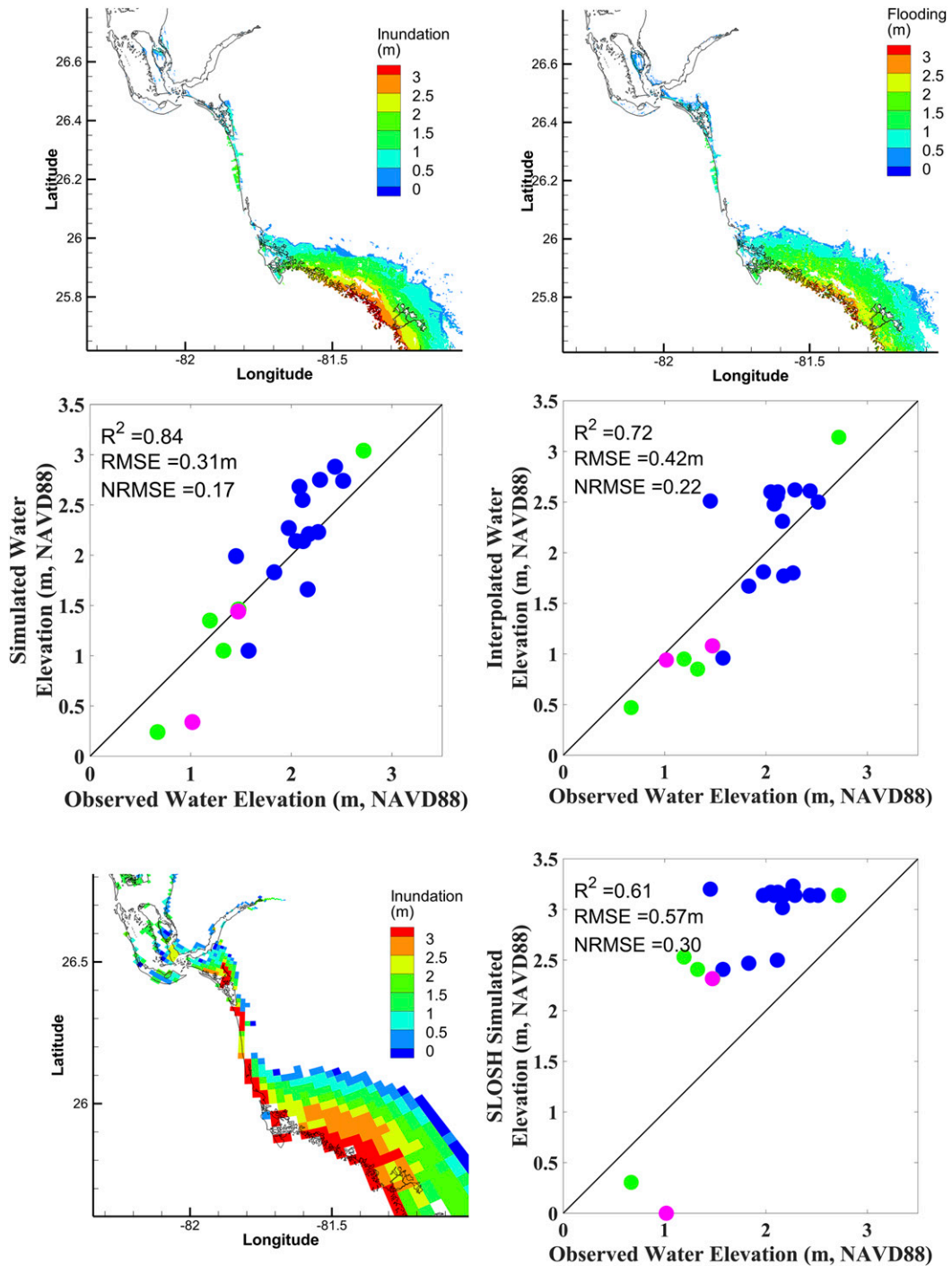


FIG. 6. As in Fig. 5, but for Hurricane Irma. Blue, green, and pink circles represent the data from USGS high water mark, USGS storm tide sensor, and NOAA tidal station, respectively.

method used by Condon et al. (2013) with the same optimal storms, as confirmed in Yang et al. (2019). The observed HWMs on Marco Island are overestimated by both direct simulation and RFMS, most likely due to the overestimated wind speed (the wind

speed at recorded at the Marco Island Airport is lower than predicted by the Holland model). The errors of HWMs in other places may be attributed to the discrepancy in topography and small-scale local features (e.g., the HWM located in a semienclosed

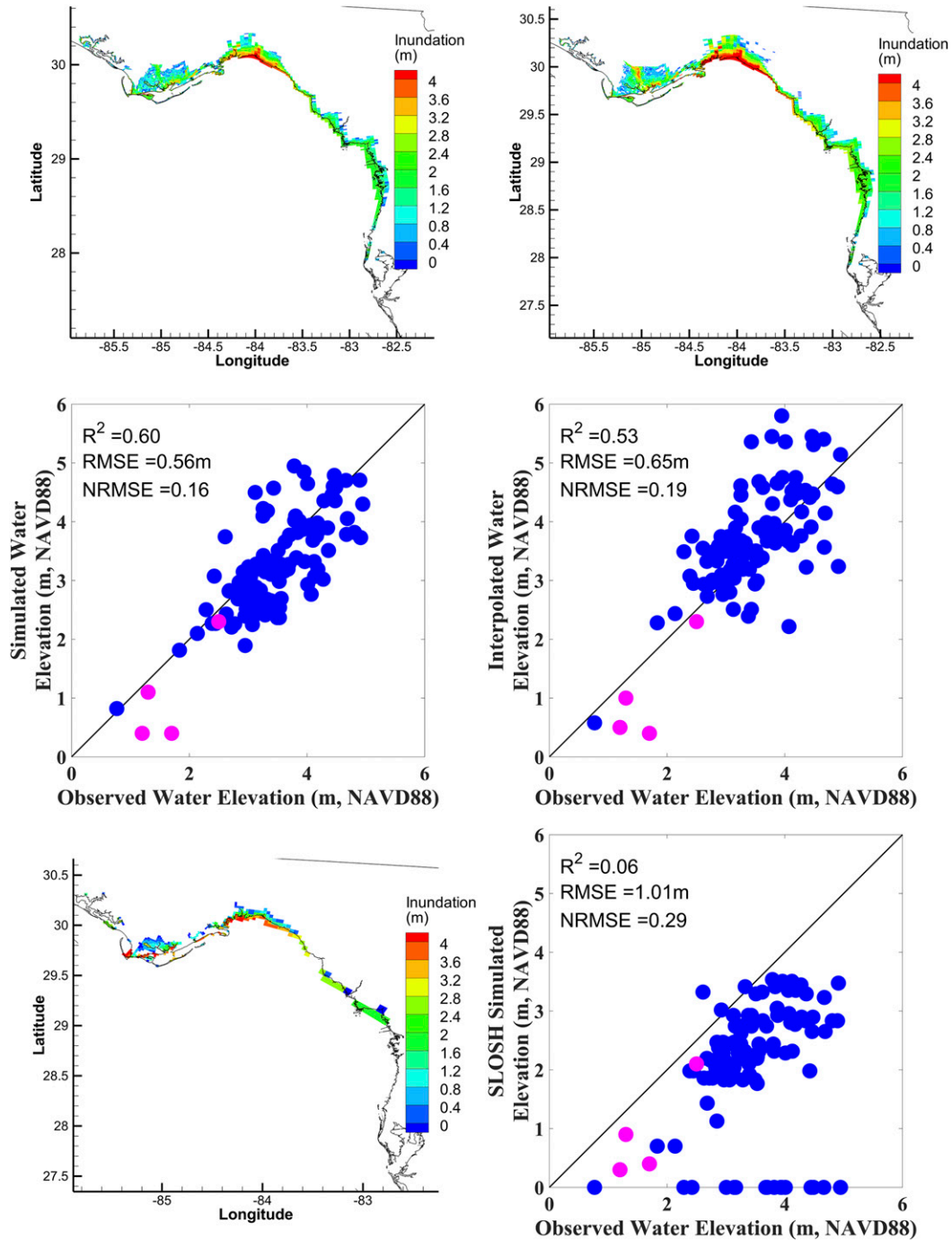


FIG. 7. As in Fig. 5, but for Hurricane Michael. Blue and pink circles represent the data from USGS high water mark and NOAA tidal station, respectively.

location) which may not be adequately resolved by the CH3D model grid.

b. Hurricane Irma (2017)

Hurricane Irma made landfall on Marco Island, Florida, as a category 3 hurricane on 10 September 2017

with the maximum wind speed of 100 mi h^{-1} . Hurricane Irma is an extremely powerful one, with the landfall parameters: P_c of 77 mb, R_m of 17.3 mi, V_f of 13.8 mi h^{-1} , θ of 0° , and L_0 of -70 (70 n mi south of CREF). Hurricane Irma is simulated by CH3D-SSMS and interpolated by the RFMS. The corresponding inundation

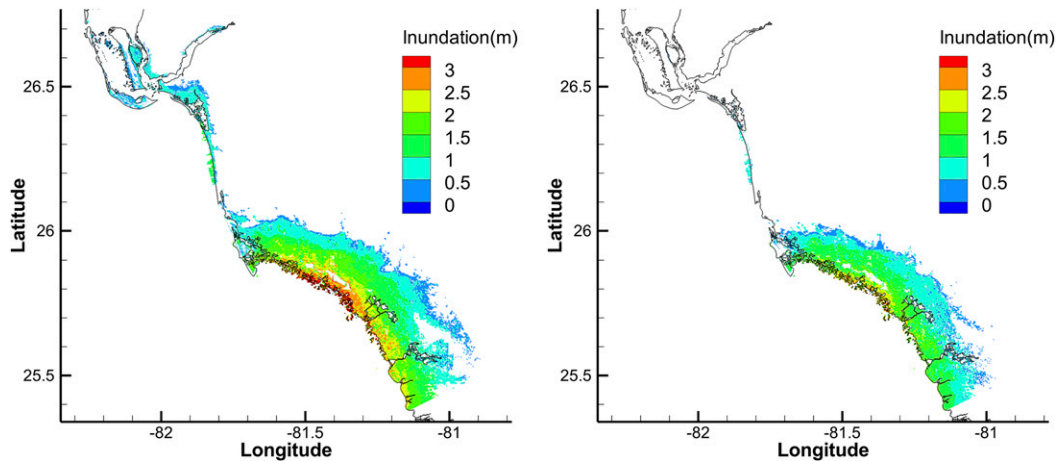


FIG. 8. Inundation maps of Hurricane Irma with uncertainty. (left) RFMS + RMSE and (right) RFMS – RMSE.

maps and the comparisons of the HWM data to the simulated and interpolated peak water levels are shown in Fig. 6. The RMSE between observed HWM data and interpolated peak water levels is 0.42 m, which is 11 cm larger than the one between observed HWM data and simulated peak water levels, with an R^2 of 0.71. The inundation map of Hurricane Irma simulated by SLOSH and the HWM comparisons are shown in Fig. 6. Overall speaking, the inundation map of Hurricane Irma by SLOSH is overestimated, with RMSE of 0.57 m and R^2 of 0.61. The large RMSE is due to the fact that the SLOSH grid is relatively coarse, hence several nearby HWM locations are within a single cell of the SLOSH domain. The CH3D domain, with a much higher resolution, can more accurately resolve these HWM locations.

The inundation area in the Collier-Seminole State Park area is overestimated by the RFMS, probably because the direct simulation uses H^*Wind , which compares better to the measured wind data than the synthetic Holland (1980) wind used by the RFMS (see Hu et al. 2012; Sheng and Zou 2017). One HWM located inside the Pumpkin Bay is overestimated by 1 m by the RFMS, probably due to interpolation error. Overall speaking, RFMS is able to forecast the storm surge of Hurricane Irma accurately (with less than 10% error in terms of ATE) and quickly.

c. Hurricane Michael (2018)

Hurricane Michael is the first category 5 hurricane that struck contiguous United States since Hurricane Andrew (1992). Hurricane Michael made landfall near Panama City within the Florida Panhandle on 10 October 2018, with the landfall parameters: P_c of 92 mb, R_m of 17.3 mi, V_f of 16.5 mi h^{-1} , θ of 33°, and L_0 of –80 (80 n mi west of CREF). Figure 7 shows the inundation maps of Hurricane Michael simulated by CH3D-SSMS and interpolated by RFMS; regression

plots of observed HWMs versus simulated peak water levels; the inundation map of Hurricane Michael simulated by SLOSH and the HWM comparisons. The simulated peak water elevations by SLOSH are underestimated compared to the observed HWMs, and some of the inland HWM locations are not inundated (simulated water elevations equal to zero), mainly due to the low grid resolution of the SLOSH domain.

The RMSE between the observed HWMs and simulated peak water levels is 0.56 m, which is 0.11 m lower than that between observed HWMs and interpolated peak water levels, with an R^2 of 0.53, compared to the R^2 of 0.06 for SLOSH. The relatively large errors at some stations can be attributed to the relatively coarse grid resolution of the Panhandle domain which (~ 800 m) is not as fine as that of the southwest Florida domain (average grid size of ~ 200 m). Thus, the inundation on small islands (e.g., St. George Island and Dog Island) and areas near some semienclosed bay (e.g., Saint Andrew Bay and Ochlockonee Bay) cannot be accurately simulated or interpolated. The results are expected to improve if finer resolution grid and topography data are used (see, e.g., Shen et al. 2006; Yin et al. 2016).

d. A sensitivity analysis

We analyzed the relative importance of the five landfall parameters in determining the TIV. In the southwest Florida domain, central pressure deficit accounts for 29% of total variability of TIV, followed by heading direction (25%), landfall location (21%), radius of maximum wind (20%), and storm forward speed (5%). In the Florida Panhandle domain, central pressure deficit accounts for 30% of total variability of TIV, followed by landfall location (22%), storm heading direction (20%), radius of maximum wind (17%) and storm forward speed (11%). These results confirm that, while pressure deficit is the most dominant

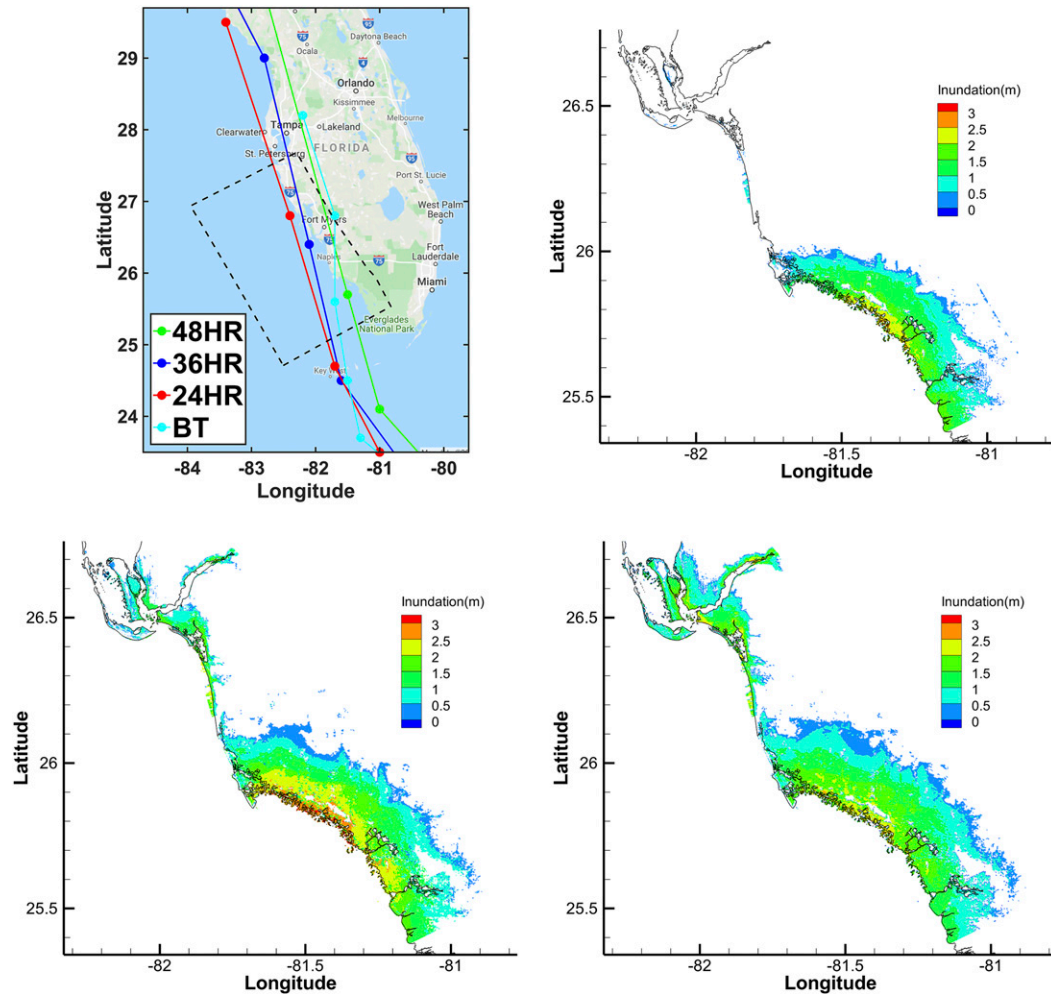


FIG. 9. (top left) Evolution of forecast tracks for Hurricane Irma, labeling corresponds to NHC forecast advisory (e.g., the label 48-HR is the forecast advisory 48 h before landfall of Hurricane Irma; BT is the best track of Hurricane Irma). (top right) Inundation map of the 48-h forecast advisory by RFMS. (bottom left) Inundation map of the 36-h forecast advisory by RFMS. (bottom right) Inundation map of the 24-h forecast advisory by RFMS.

parameter in affecting coastal inundation during hurricanes considered in this study, other factors such as radius to maximum wind, heading direction, landfall location, and storm speed also play very significant roles hence cannot be de-emphasized. The NHC website used to relate surge height to hurricane intensity [represented by the Saffir-Simpson Hurricane Wind scale (<https://www.nhc.noaa.gov/aboutsshws.php>)] only, but that has been removed after Hurricane Katrina, which demonstrated that surge and flood depend significantly on the other parameters (hurricane size, forward speed, heading direction, and landfall location) as well. Our sensitivity analysis confirms that.

5. Uncertainty analysis of kriging interpolation

The uncertainty of kriging interpolation method used in this study can be directly estimated by the RFMS,

since the RMSE of every grid cell inside the domain is calculated using the spatial correlation coefficients [see Lophaven et al. (2002) and Yang et al. (2019) for details]. The uncertainty depends on the input landfall parameters and the simulated water level responses of the optimal storms and varies from place to place inside the domain.

For a single storm prediction, the RFMS calculates the interpolated water level and RMSE for every cell inside the domain. The upper limit of predicted water level is calculated as interpolated water level (denoted as RFMS) plus RMSE: $(\text{RFMS} + \text{RMSE})$, and the lower limit of predicted water level is calculated as interpolated water level minus RMSE: $(\text{RFMS} - \text{RMSE})$. The inundation maps of Hurricane Irma with uncertainty considered are shown in Fig. 8 as an example.

The inundation area is increased by 35% in the upper-limit case, and Sanibel Island and Pine Island, which are barely inundated in the inundation map without uncertainty (Fig. 6), are inundated. For Everglades National Park, the maximum inundation height is increased by 40 cm, with the inundation area increased by 10%. The lower limit case shows 23% decrease of inundation area and lower inundation heights. In practice, the upper-limit case is more useful as it could provide the extreme condition to be used by the emergency managers of local government for hurricane response and mitigation planning.

6. RFMS using forecast advisories

One of the challenges in forecasting storm surge is the abrupt change in forecast advisory issued by NHC, such as the forecast advisories of Hurricane Charley and Hurricane Irma. Hurricane Charley was forecasted to landfall near Tampa Bay, but it shifted over 60 mi to the south in the final advisory only 12 h before landfall (Pasch et al. 2004; Condon et al. 2013). Hurricane Irma was predicted to make landfall at Everglades City according to the forecast advisory 48 h before landfall. Twenty-four hours later, the forecasted landfall location shifted 100 mi to the north at Sarasota. As shown in the best track (Fig. 9), the landfall location moved 80 mi back to the south at Macro Island. Such sudden changes of forecast advisory require the storm surge forecast system to respond quickly (in a few minutes) to update the inundation map, which poses a major challenge for any high-resolution real-time storm surge forecast system introduced earlier in the paper. In such occasions, the RFMS presented in this paper can be extremely useful.

Figure 9 shows the inundation maps produced by the RFMS using the 48-, 36- and 24-h forecast advisories. Figure 10 shows the RMSE for SLOSH and RFMS for different forecast cycles. Overall, the RFMS performs better than SLOSH when compared to the observed data. The TIV and total inundation area of the inundation map for the 24-h forecast advisory are increased by over 100% compared to those for the 48-h forecast advisory. This shows that abrupt change of forecast advisory can greatly alter the inundation volume and area influenced by the hurricane. The RFMS, which is capable of generating a high-resolution inundation map from the new storm advisory in 1 min, can enable the emergency managers to modify the evacuation plan quickly.

The tropical cyclone forecast models used by the NHC, including dynamical models, statistical models, and statistical–dynamical models, produce a number of

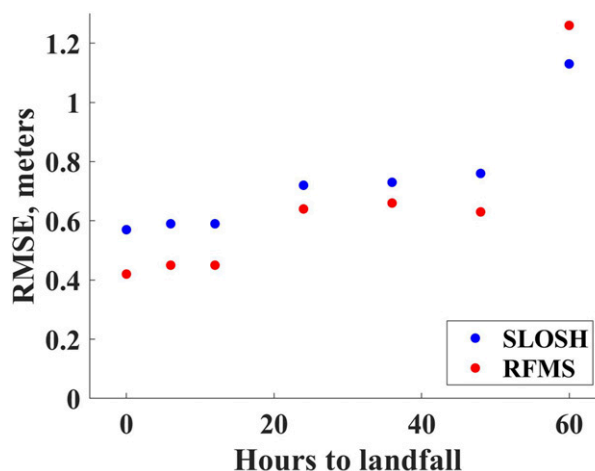


FIG. 10. RMSE of simulated vs observed data (observation include the data from USGS high water mark and NOAA tidal stations) for SLOSH and RFMS.

forecast advisories within a forecast cycle (NHC 2009). The uncertainty of the estimated landfall parameters depends on the forecast advisories, whose errors are discussed in detail in Condon et al. (2013) and Landsea and Franklin (2013). The forecast advisories are used by the RFMS to generate a comprehensive inundation map for each forecast cycle, as described below.

- 1) Find the forecasts that will make landfall at the study domain.
- 2) Estimate the landfall parameters from the forecasts, which are used by RFMS to calculate the corresponding inundation maps.
- 3) For each land cell inside the domain, count the number of storms N that have inundation greater than 1ft at that cell.
- 4) Compute the inundation probability as $N/\text{total number of forecast advisories}$.
- 5) Plot the map of inundation probability as a comprehensive inundation map.

Figure 11 shows forecast advisories issued by NHC 48 h before landfall and the corresponding comprehensive inundation map. There were 73 advisories issued by NHC, 54 of which were predicted to make landfall on the southwest Florida domain. The central pressure and radius to maximum wind data are missing for some of the forecasts, and the data from the official forecast (OFCL) are used instead. The comprehensive inundation map was completed in 1 min (reference system Intel Core i7–6700). Since the probabilistic inundation map incorporates all forecast advisories and their uncertainties, it contains much more informative than a single inundation map, hence is more useful for the local emergency managers. The inundation probability and

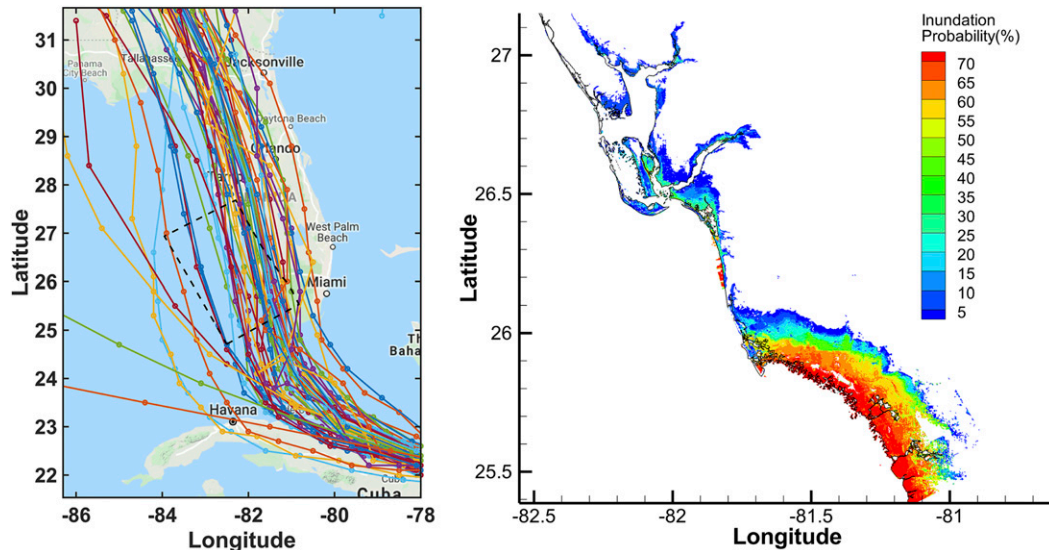


FIG. 11. (left) The forecast advisories of Hurricane Irma issued by NHC 48 h before landfall. (right) The comprehensive inundation map of Hurricane Irma at 48 h before landfall.

the corresponding severity of the inundation threat are described in Table 2.

The uncertainty of the RFMS due to the storm forecast errors could be estimated by using the forecast advisories issued by NHC. At each forecast cycle (6 h), the storm advisories are used by RFMS to generate the inundation maps. The inundation values are ranked from lowest to the highest, and the 5th and 95th percentiles of inundations are calculated accordingly at each location. The forecast advisories at 47 and 5 h before the landfall of Hurricane Michael are used and the comparisons of observed HWMs and interpolated HWMs by RFMS with uncertainties are shown in Figs. 12c and 12d. As noted by NHC (Brown 2017): “We (NHC) still have significant difficulty in forecasting rapidly intensifying and rapidly weakening storms.” The central pressure deficit predictions of Hurricane Michael, a rapidly intensified storm, were generally lower than the best track values, thus resulting in the lower predicted HWMs and the relatively large vertical uncertainties which is a measure of the uncertainties associated with the pressure deficit predicted by various atmospheric models.

To confirm that the uncertainties shown in Figs. 12c and 12d represent the uncertainties associated with the tropical cyclone forecast models used by NHC, but not a measure of the uncertainties of the RFMS, the RFMS was ran by setting the central pressure deficit values of all track advisories for Hurricane Michael to the values of the best track at 47 and 5 h prior to landfall. This eliminates the uncertainty caused by the underestimation of storm intensity. Figures 12e and 12f show the new HWM comparisons with less vertical

uncertainty. This shows that if and when NHC improves their prediction of storm intensity and size, the RFMS predicted HWMs would become much more accurate.

7. Summary and conclusions

This paper introduces an accurate and efficient rapid forecast and mapping system (RFMS) of hurricane-induced storm surge and coastal flooding. It uses the quick kriging interpolation method with the storm surge database consisting of high-fidelity simulations of the optimal storms and can generate high-resolution storm surge response and inundation map for an approaching hurricane or a “what-if” scenario in 1 min. An objective method for selecting the optimal storms for RFMS is proposed and evaluated by selecting 490 optimal storms for southwest Florida and Florida Panhandle. For an approaching hurricane, five landfall parameters (center pressure deficit, radius to maximum wind, storm forward speed, storm heading direction, and landfall location) are calculated from National Hurricane Center forecast advisory and used by the RFMS to predict the storm surge and inundation map. The RFMS presents

TABLE 2. The inundation probability and the corresponding inundation threat.

Inundation probability	Inundation threat
>50%	Very high
30%–50%	High
10%–30%	Moderate
<10%	Low

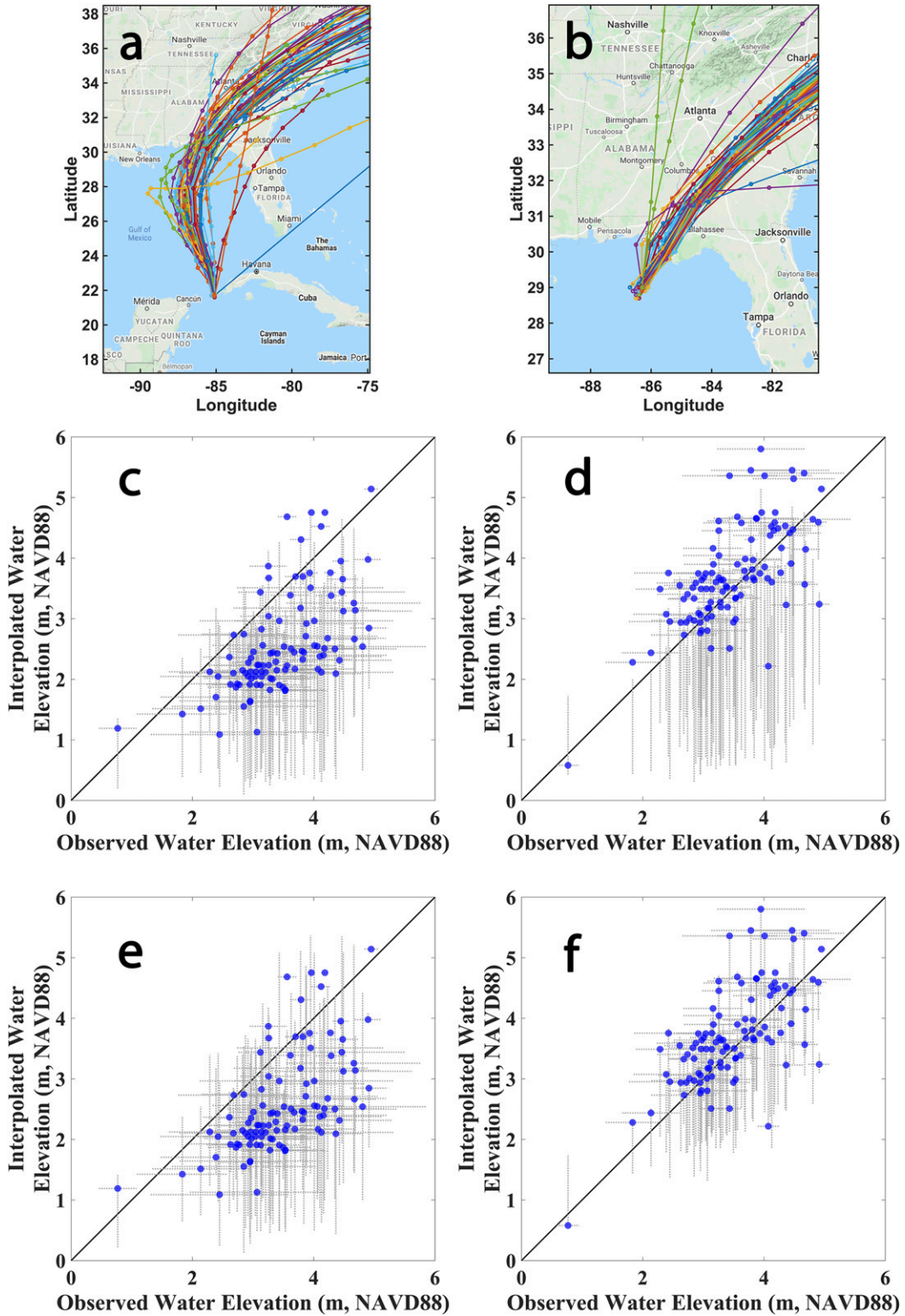


FIG. 12. Forecast advisories of Hurricane Michael issued by NHC at (a) 47 and (b) 5 h before landfall. HWM comparisons between observed HWMs and interpolated HWMs by RFS using the forecast advisories at (c) 47 and (d) 5 h before landfall, and using the forecast advisories with central pressure deficit values replaced by the values from the best track at (e) 47 and (f) 5 h before landfall. The horizontal gray lines of HWM comparisons indicate the uncertainties calculated by kriging algorithm, and the vertical gray lines indicate the 5th and 95th percentiles of HWM predictions by RFMS.

an attractive alternative for producing very quick and accurate surge and inundation forecast and map without direct model forecasting, which requires excessive computing resources.

The key findings of this paper are as follows:

- 1) The RFMS that uses the quick kriging interpolation method is highly efficient. It takes about 1 min to produce high-fidelity forecast and inundation map during an approaching storm or “what-if” scenario using only a single CPU.
- 2) The RFMS is validated for Hurricanes Charley, Irma, and Michael on two different domains in Florida. The coefficients of determination (R^2) between observed and simulated (by CH3D-SSMS) high water marks (HWMs) for the three hurricanes are between 0.60 and 0.84, with the root-mean-square error (RMSE) from 0.31 to 0.56 m. While the coefficients of determination between observed and interpolated HWMs by RFMS for the three hurricanes are between 0.53 and 0.72, with RMSE from 0.37 to 0.65 m. The comparisons show that the RFMS is capable of generating a sufficiently accurate high-resolution inundation map of an approaching storm in 1 min. With similar amount of computing time, RFMS could generate much higher resolution and more accurate inundation maps than SLOSH. The detailed coastal inundation maps can be used as supplement to the lower-resolution SLOSH forecast.
- 3) The uncertainties of the RFMS can be estimated and added to the predicted inundation maps to provide the extreme flood condition to be considered by the emergency managers of local governments for evacuation and mitigation planning.
- 4) When a forecast advisory shows sudden unexpected changes of landfall parameters, the RFMS can quickly generate a flood forecast and inundation map. This is very useful during such hurricanes as Charley and Irma whose tracks changed abruptly after a forecast advisory is issued, or in Hurricane Harvey and Michael which underwent rapid intensification due to a very warm ocean.
- 5) The forecast advisories from the tropical cyclone forecast models by the NHC could be used by the RFMS to quantify the uncertainty of predicted storm surge due to the storm forecast errors. The RFMS can provide accurate prediction of the storm surge with uncertainties if accurate storm forecasts are provided by NHC in the future.

The RFMS introduced in this study is a prototype system that focuses on the methodology of quickly forecasting the storm surge and inundation using surrogate modeling. The forecasting results could be improved by including the effects of the precipitation, river flow and

vegetation, though the current RFMS already could generate more accurate storm surge and inundation forecast than SLOSH. The effect of precipitation could be included by coupling with the hurricane rainfall model such as the Parametric Hurricane Rainfall Model (PHRAM; see [Lonfat et al. 2007](#)), or the tropical cyclone rain rate model of [Snaiki and Wu \(2018\)](#). The river flow and inland flooding could be accounted for by coupling with the hydrologic model such as the Coupled Routing and Excess Storage model (CREST; [Blanton et al. 2018](#)), or the Gridded Surface/Subsurface Hydrologic Analysis model (GSSHA; [Silva-Araya et al. 2018](#)).

The 3D vegetation-resolving surge model ([Sheng et al. 2012b](#); [Sheng and Zou 2017](#)), instead of the 2D surge model in this study, could be used to improve the simulation of water levels and waves in vegetated areas. The Manning’s coefficients of the vegetated areas such as the Everglades National Park are derived from the land cover data, which does not consider vegetation’s density, height, and vertical structure, and could result in errors (see, e.g., [Lapetina and Sheng 2014](#); [Medeiros et al. 2015](#); [Sheng and Zou 2017](#)). Moreover, incorporating the high-resolution LiDAR data into the digital elevation model (DEM) could increase the resolution of near-shore topography data, which improves the accuracy of flooding forecast (see, e.g., [Blumberg et al. 2015](#)).

To further improve the accuracy of the RFMS, the dynamic surge model could be enhanced. For example, the 3D vegetation-resolving CH3D-SSMS can be used instead of the 2D version used in this study. CH3D-SSMS can be coupled to stormwater model and watershed model to include the effects of precipitation, freshwater, and groundwater on coastal inundation. While the expanded dynamic modeling system will increase the computing time it takes to develop simulations of the optimal storms, the resulting RFMS will still take only 1–3 min to produce a forecast of coastal inundation map. The RFMS technology will also allow the quick and frequent revision of flood maps, which now takes more than five years. For example, after every hurricane season, flood map for any coastal region could be quickly revised by adding the new storm data to the RFMS preprocessing step to revise the optimal storm database.

Acknowledgments. This paper is a result of research funded by the National Oceanic and Atmospheric Administration’s RESTORE Science Program under Award NA17NOS4510094 to the University of Florida, as well as research funded by Florida Sea Grant (R/C-S-59), NOAA Climate Program Office Grant NO11OAR4310105, and SECOORA/NOAA/NOPP [IOOS.11(033)UF.PS.MOD.1]. The authors thank two anonymous reviewers for their valuable comments.

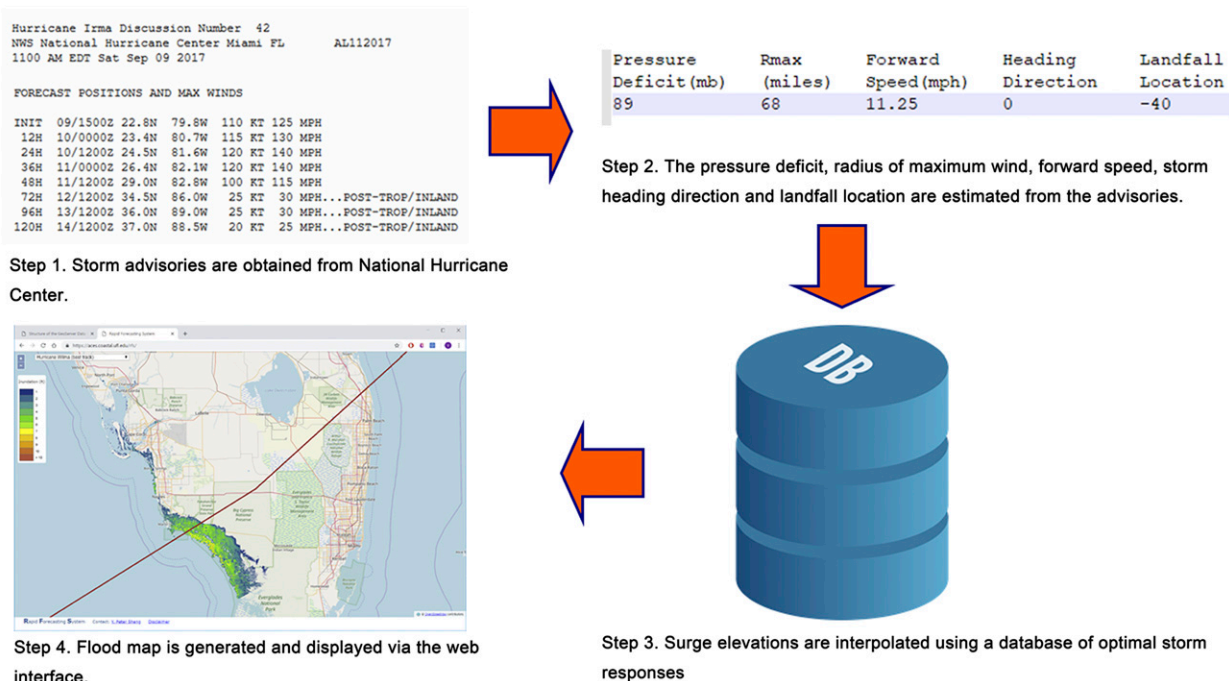


FIG. C1. Forecasting procedure of RFMS.

APPENDIX A

Southwest Florida Domains

The southwest Florida domain of CH3D model covers approximately 170 mi alongshore, from Ponce De Leon Bay on the south to the Palma Sola Bay on the north, and the domain's cross-shore coverage is around 115 mi (90 mi offshore and 25 mi inland). The study domain has relatively mild slope (compared to southeast Florida), with the water depth increasing to 100 m at the offshore boundary. The cities such as Sarasota, Fort Myers, and Naples and six counties are included in the domain. The CH3D domain has 386 140 cells with a minimum resolution of 20 m in coastal areas and average grid size of about 200 m. The southwest Florida domain of the SLOSH model ("efm2") extends farther south to the Florida Keys and has less coverage in Bradenton, Florida, compared to that of the CH3D model. The SLOSH grid has 11 100 cells and a minimum resolution of ~200 m and an average grid size of ~1500 m.

APPENDIX B

Florida Panhandle Domains

The Florida Panhandle domain of CH3D model covers about 300 mi alongshore, from Pensacola to Clearwater. The domain covers about 40 000 mi² of northeastern Gulf of Mexico and extends 15–20 mi inland from the coastline.

A total of 16 counties of Florida are included in the domain. The CH3D domain has 131 560 cells with a minimum resolution of ~150 m in coastal areas and averaged grid size of ~800 m. The Florida domain of the SLOSH model ("ap3") covers similar areas with that of CH3D model, except the Tampa Bay area is not included. The SLOSH grid has 6603 cells and average grid size of ~3000 m. Both the southwest Florida domain and Florida Panhandle domain of CH3D have significantly higher spatial resolution, compared to those of SLOSH.

APPENDIX C

Forecasting Procedure of RFMS

The forecasting procedure of RFMS described in section 3d is shown in Fig. C1.

REFERENCES

- Bao, S., L. Xie, and L. J. Pietrafesa, 2006: An asymmetric hurricane wind model for storm surge and wave forecasting. *27th Conf. on Hurricanes and Tropical Meteorology*, Monterey, CA, Amer. Meteor. Soc., 9A.4, http://ams.confex.com/ams/27Hurricanes/techprogram/paper_107653.htm.
- Blake, E., C. W. Landsea, and E. J. Gibney, 2011: The deadliest, costliest, and most intense United States tropical cyclones from 1851 to 2010 (and other frequently requested hurricane facts). NOAA Tech. Memo. NWS NHC-6, 47 pp., <http://www.nhc.noaa.gov/pdf/nws-nhc-6.pdf>.

- Blanton, B., and Coauthors, 2018: An integrated scenario ensemble-based framework for hurricane evacuation modeling: Part 2—Hazard modeling. *Risk Anal.*, **40**, 117–133, <https://doi.org/10.1111/RISA.13004>.
- Blumberg, A. F., N. Georgas, L. Yin, T. O. Herrington, and P. M. Orton, 2015: Street-scale modeling of storm surge inundation along the New Jersey Hudson River waterfront. *J. Atmos. Oceanic Technol.*, **32**, 1486–1497, <https://doi.org/10.1175/JTECH-D-14-00213.1>.
- Booij, N., R. C. Ris, and L. H. Holthuijsen, 1999: A third-generation wave model for coastal regions: 1. Model description and validation. *J. Geophys. Res.*, **104**, 7649–7666, <https://doi.org/10.1029/98JC02622>.
- Brown, D., 2017: Tropical cyclone intensity forecasting: Still a challenging proposition. National Hurricane Center, 29 pp., https://www.nhc.noaa.gov/outreach/presentations/NHC2017_IntensityChallenges.pdf.
- Chen, C., H. Liu, and R. C. Beardsley, 2003: An unstructured grid, finite-volume, three-dimensional, primitive equations ocean model: Application to coastal ocean and estuaries. *J. Atmos. Oceanic Technol.*, **20**, 159–186, [https://doi.org/10.1175/1520-0426\(2003\)020<0159:AUGFVT>2.0.CO;2](https://doi.org/10.1175/1520-0426(2003)020<0159:AUGFVT>2.0.CO;2).
- Condon, A. J., and Y. P. Sheng, 2012: Optimal storm generation for evaluation of the storm surge inundation threat. *Ocean Eng.*, **43**, 13–22, <https://doi.org/10.1016/j.oceaneng.2012.01.021>.
- , —, and V. A. Paromygin, 2013: Towards high-resolution, rapid, probabilistic forecasting of the inundation threat from landfalling hurricanes. *Mon. Wea. Rev.*, **141**, 1304–1323, <https://doi.org/10.1175/MWR-D-12-00149.1>.
- FEMA, 2019: Base flood elevation. Accessed 1 November 2019, <https://www.fema.gov/base-flood-elevation>.
- Fleming, J., C. Fulcher, R. A. Luettich, B. Estrade, G. Allen, and H. Winer, 2008: A real time storm surge forecasting system using ADCIRC. *Proc. 10th Int. Conf. on Estuarine and Coastal Modeling X*, Newport, RI, ASCE, 373–392.
- Forbes, C., J. Rhome, C. Mattocks, and A. Taylor, 2014a: Prediction and verification of storm surge during Hurricane Sandy with the NWS SLOSH model. *31st Conf. on Hurricanes and Tropical Meteorology*, San Diego, CA, Amer. Meteor. Soc., 2D.5, <https://ams.confex.com/ams/31Hurr/webprogram/Paper244123.html>.
- , —, —, and —, 2014b: Predicting the storm surge threat of Hurricane Sandy with the National Weather Service SLOSH model. *J. Mar. Sci. Eng.*, **2**, 437–476, <https://doi.org/10.3390/jmse2020437>.
- Holland, G., 1980: An analytic model of the wind and pressure profiles in hurricanes. *Mon. Wea. Rev.*, **108**, 1212–1218, [https://doi.org/10.1175/1520-0493\(1980\)108<1212:AAMOTW>2.0.CO;2](https://doi.org/10.1175/1520-0493(1980)108<1212:AAMOTW>2.0.CO;2).
- Hu, K., Q. Chen, and S. K. Kimball, 2012: Consistency in hurricane surface wind forecasting: An improved parametric model. *Nat. Hazards.*, **61**, 1029–1050, <https://doi.org/10.1007/s11069-011-9960-z>.
- Irish, J. L., D. T. Resio, and J. Ratcliff, 2008: The influence of storm size on hurricane surge. *J. Phys. Oceanogr.*, **38**, 2003–2013, <https://doi.org/10.1175/2008JPO3727.1>.
- Jelesnianski, C. P., J. Chen, and W. A. Shaffer, 1992: SLOSH: Sea, lake, and overland surges from hurricanes. NOAA Tech. Rep. NWS-48, U.S. Department of Commerce, National Oceanic and Atmospheric Administration, National Weather Service, Silver Spring, MD, 71 pp.
- Jia, G., A. A. Taflanidis, N. C. Norterto, J. Melby, A. Kennedy, and J. Smith, 2016: Surrogate modeling for peak or time-dependent storm surge prediction over an extended coastal region using an existing database of synthetic storm. *Nat. Hazards.*, **81**, 909–938, <https://doi.org/10.1007/s11069-015-2111-1>.
- Jordan, M. R., and C. A. Clayson, 2008: Evaluating the usefulness of a new set of hurricane classification indices. *Mon. Wea. Rev.*, **136**, 5234–5238, <https://doi.org/10.1175/2008MWR2449.1>.
- Jordi, A., and Coauthors, 2019: A next-generation coastal ocean operational system: Probabilistic flood forecasting at street scale. *Bull. Amer. Meteor. Soc.*, **100**, 41–54, <https://doi.org/10.1175/BAMS-D-17-0309.1>.
- Kim, S.-W., J. Melby, N. Nadal-Caraballo, and J. Ratcliff, 2015: A time-dependent surrogate model for storm surge prediction based on an artificial neural network using high-fidelity synthetic hurricane modeling. *Nat. Hazards.*, **76**, 565–585, <https://doi.org/10.1007/s11069-014-1508-6>.
- Landsea, C. W., and J. L. Franklin, 2013: Atlantic hurricane database uncertainty and presentation of a new database format. *Mon. Wea. Rev.*, **141**, 3576–3592, <https://doi.org/10.1175/MWR-D-12-00254.1>.
- Lapetina, A., and Y. P. Sheng, 2014: Three-dimensional modeling of storm surge and inundation including the effects of coastal vegetation. *Estuaries Coasts*, **37**, 1028–1040, <https://doi.org/10.1007/s12237-013-9730-0>.
- Lonfat, M., R. Rogers, T. Marchok, and F. D. Marks, 2007: A parametric model for predicting hurricane rainfall. *Mon. Wea. Rev.*, **135**, 3086–3097, <https://doi.org/10.1175/MWR3433.1>.
- Lophaven, S. N., H. B. Nielsen, and J. Sondergaard, 2002: Aspects of the Matlab toolbox DACE. Informatics and Mathematical Modelling Rep. IMM-REP-2002-13, Technical University of Denmark, Kongens Lyngby, Denmark, 44 pp.
- Luettich, R. A., J. J. Westerink, and N. W. Scheffner, 1992: ADCIRC: An advanced three-dimensional circulation model for shelves, coasts, and estuaries. Rep. 1, Theory and methodology of ADCIRC-2DDI and ADCIRC-3DL. Tech. Rep. DRP-92-6, U.S. Army Engineer Waterways Experiment Station, Vicksburg, MS, 137 pp.
- Mattocks, C., and C. Forbes, 2008: A real-time, event-triggered storm surge forecasting system for the state of North Carolina. *Ocean Modell.*, **25**, 95–119, <https://doi.org/10.1016/j.ocemod.2008.06.008>.
- Medeiros, S. C., S. C. Hagen, and J. Weishampel, 2015: A random forest model based on lidar and field measurements for parameterizing surface roughness in coastal modeling. *IEEE J. Sel. Top. Appl. Earth Obs. Remote Sens.*, **8**, 1582–1590, <https://doi.org/10.1109/JSTARS.2015.2419817>.
- NHC, 2009: Technical summary of the National Hurricane Center track and intensity models. National Oceanic and Atmospheric Administration, 18 pp., https://www.nhc.noaa.gov/pdf/model_summary_20090724.pdf.
- , 2019: Storm Surge Maximum of the Maximum (MOM). Accessed 1 November 2019, <https://www.nhc.noaa.gov/surge/momDescrip.php>.
- NOAA/NWS/NHC, 2013: Sea, Lake, and Overland Surge from Hurricanes (SLOSH). Accessed 23 January 2019, <http://www.nhc.noaa.gov/surge/slosh.php>.
- NRC, 2009: Mapping the zone—Improving flood map accuracy. National Research Council of the National Academies, Committee on FEMA flood maps, National Academies Press, 136 pp.
- Pasch, R. J., D. P. Brown, and E. S. Blake, 2004: Tropical Cyclone Report: Hurricane Charley (9–14 August 2004). National Hurricane Center, 23 pp., https://www.nhc.noaa.gov/data/tcr/AL032004_Charley.pdf.
- Paromygin, V. A., Y. P. Sheng, and J. R. Davis, 2017: Towards the development of an operational forecast system for the Florida

- coast. *J. Mar. Sci. Eng.*, **5**, 8, <https://doi.org/10.3390/jmse5010008>.
- Peng, M., L. Xie, and L. J. Pietrafesa, 2004: A numerical study of storm surge and inundation in the Croatan–Albemarle–Pamlico Estuary System. *Estuarine Coastal Shelf Sci.*, **59**, 121–137, <https://doi.org/10.1016/j.ecss.2003.07.010>.
- Powell, M. D., S. H. Houston, L. R. Amat, and N. Morisseau-Leroy, 1998: The HRD real-time hurricane wind analysis system. *J. Wind Eng. Ind. Aerodyn.*, **77–78**, 53–64, [https://doi.org/10.1016/s0167-6105\(98\)00131-7](https://doi.org/10.1016/s0167-6105(98)00131-7).
- Powers, J. G., and Coauthors, 2017: The Weather Research and Forecasting Model: Overview, system efforts, and future directions. *Bull. Amer. Meteor. Soc.*, **98**, 1717–1737, <https://doi.org/10.1175/BAMS-D-15-00308.1>.
- Rego, D. T., and C. Li, 2009: On the importance of the forward speed of hurricanes in storm surge forecasting: A numerical study. *Geophys. Res. Lett.*, **36**, L07609, <https://doi.org/10.1029/2008GL036953>.
- Shen, J., K. Zhang, C. Xiao, and W. Gong, 2006: Improved prediction of storm surge inundation with a high-resolution unstructured grid model. *J. Coastal Res.*, **22**, 1309–1319, <https://doi.org/10.2112/04-0288.1>.
- Sheng, Y. P., 1987: On modeling three-dimensional estuarine and marine hydrodynamics. *Three-Dimensional Models of Marine and Estuarine Dynamics*, J. C. J. Nihoul and B. M. Jamart, Eds., Elsevier Oceanography Series, Elsevier, 35–54.
- , 1990: Evolution of a three-dimensional curvilinear-grid hydrodynamic model for estuaries, lakes and coastal waters: CH3D. *Estuarine and Coastal Modeling: Proc. Estuarine and Coastal Circulation and Pollutant Transport Model Data Comparison Specialty Conf.*, Reston, VA, ASCE, 40–49.
- , and R. Zou, 2017: Assessing the role of mangrove forest in reducing coastal inundation during major hurricane. *Hydrobiologia*, **803**, 87–103, <https://doi.org/10.1007/s10750-017-3201-8>.
- , V. A. Paramygin, V. Alymov, and J. R. Davis, 2006: A real-time forecasting system for hurricane induced storm surge and coastal flooding. *Proc. Ninth Int. Conf. on Estuarine and Coastal Modeling*, Reston, VA, ASCE, 585–602.
- , Y. Zhang, and V. A. Paramygin, 2010: Simulation of storm surge, wave, currents and inundation in the Outer Banks and Chesapeake Bay during Hurricane Isabel in 2003: The importance of waves. *J. Geophys. Res.*, **115**, C04008, <https://doi.org/10.1029/2009JC005402>.
- , and Coauthors, 2012a: A regional testbed for storm surge and coastal inundation models—An overview. *Proc. Int. Conf. on Estuarine and Coastal Modeling (2011)*, St. Augustine, FL, ASCE, 476–495.
- , A. Lapetina, and G. Ma, 2012b: The reduction of storm surge by vegetation canopies: Three-dimensional simulations. *Geophys. Res. Lett.*, **39**, L20601, <https://doi.org/10.1029/2012GL053577>.
- Silva-Araya, W. F., F. L. Santiago-Collazo, J. Gonzalez-Lopez, and J. Maldonado-Maldonado, 2018: Dynamic modeling of surface runoff and storm surge during hurricane and tropical storm events. *Hydrology*, **5**, 13, <https://doi.org/10.3390/hydrology5010013>.
- Snaiki, R., and T. Wu, 2018: An analytical framework for rapid estimate of rain rate during tropical cyclones. *J. Wind Eng. Ind. Aerodyn.*, **174**, 50–60, <https://doi.org/10.1016/j.jweia.2017.12.014>.
- Sugarbaker, L. J., and W. J. Carswell, 2011: *The national map. U.S. Geological Survey Fact Sheet (2011)*, 2011–3042.
- Vickery, P. J., P. F. Skerlj, and L. A. Twisdale, 2000: Simulation of hurricane risk in the U.S. using empirical track model. *J. Struct. Eng.*, **126**, 1222–1237, [https://doi.org/10.1061/\(ASCE\)0733-9445\(2000\)126:10\(1222\)](https://doi.org/10.1061/(ASCE)0733-9445(2000)126:10(1222)).
- Wikipedia, 2019: List of Florida hurricanes. Accessed 6 January 2019, https://en.wikipedia.org/wiki/List_of_Florida_hurricanes.
- Xie, L., S. Bao, L. J. Pietrafesa, K. Foley, and M. Fuentes, 2006: A real-time hurricane surface wind forecasting model: Formulation and verification. *Mon. Wea. Rev.*, **134**, 1355–1370, <https://doi.org/10.1175/MWR3126.1>.
- Yang, K., V. A. Paramygin, and Y. P. Sheng, 2019: An objective and efficient method for estimating probabilistic coastal inundation hazards. *Nat. Hazards*, **99**, 1105–1130, <https://doi.org/10.1007/s11069-019-03807-w>.
- Yin, J., N. Lin, and D. Yu, 2016: Coupled modeling of storm surge and coastal inundation: A case study in New York City during Hurricane Sandy. *Water Resour. Res.*, **52**, 8685–8699, <https://doi.org/10.1002/2016WR019102>.